

PSK Demodulation (Part 2)

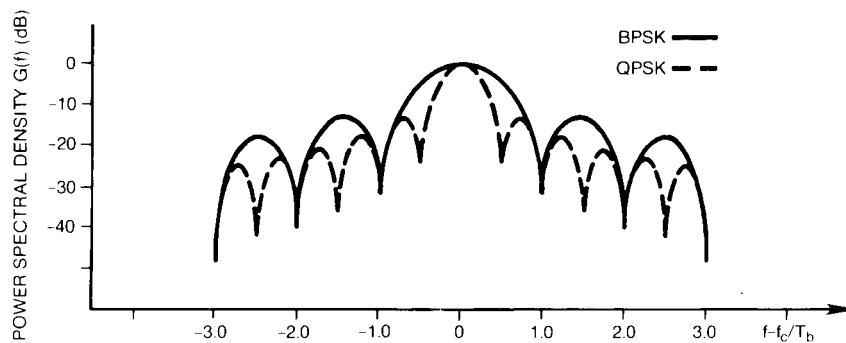
J. Mark Steber

Symbol Timing Recovery

The second subsection required for PSK demodulation is the *symbol timing recovery*, or STR circuitry. All techniques discussed here are data-derived; i.e., the timing information required to optimize for correct bit decisions is derived from the raw data itself. Additionally, only suboptimal techniques will be discussed. Optimal techniques developed for deep space telemetry applications [3] can be slow in acquisition when used for burst-mode modem operation, and are difficult and costly to implement.

Ideally, the STR circuitry provides clock pulses to the bit sampler at the midpoint between data transitions; i.e., in the middle of each bit's time slot. The STR tracks any fluctuation in frequency and/or phase due to transmitting clock oscillator drift or jitter.

The typical STR used in uncoded PSK systems is comprised of two blocks; a nonlinear element and a narrowband filter, as is shown in Figure 1. Consider the typical case in which the raw data are formatted as non-return to zero (NRZ) pulses. An NRZ pulse can assume either of two allowable levels, and is held there for the duration of the signaling interval [11]. The power spectral density for such a bipolar NRZ data stream takes the form of that shown in Figure 1, Part 1, for BPSK, shifted down to $f_c = 0$ [The figure is repeated below for convenience. -Ed.]



Part 1, Figure 1. BPSK and QPSK spectra.

With a spectral null at the symbol frequency, nonlinear processing is required to extract timing information; that is, to generate spectral lines at multiples of the symbol rate. The narrowband filter then tracks the line at

$$f = 1/T_s$$

The residual lines contribute to the recovered clock jitter.

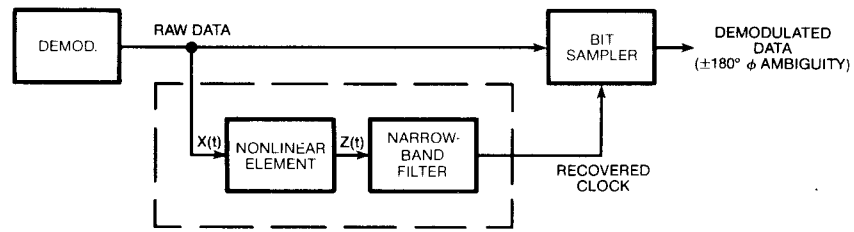


Figure 1. Block diagram of symbol timing recovery.

The nonlinearity can be implemented in many forms, such as a differentiator, a squarer, a delay and multiply circuit, or a threshold detector. Typically, the methods shown in Figure 2 have gained favor due to their simplicity and low cost. Versions A and B are equivalent, and analyzed by Feher [12]. They are primarily low-to-moderate speed realizations, but can be used in systems where the baud rate approaches the switching limits of the digital hardware, roughly 10 Mbs. Version C, a delay and multiply technique, is preferred for high-speed application [11].

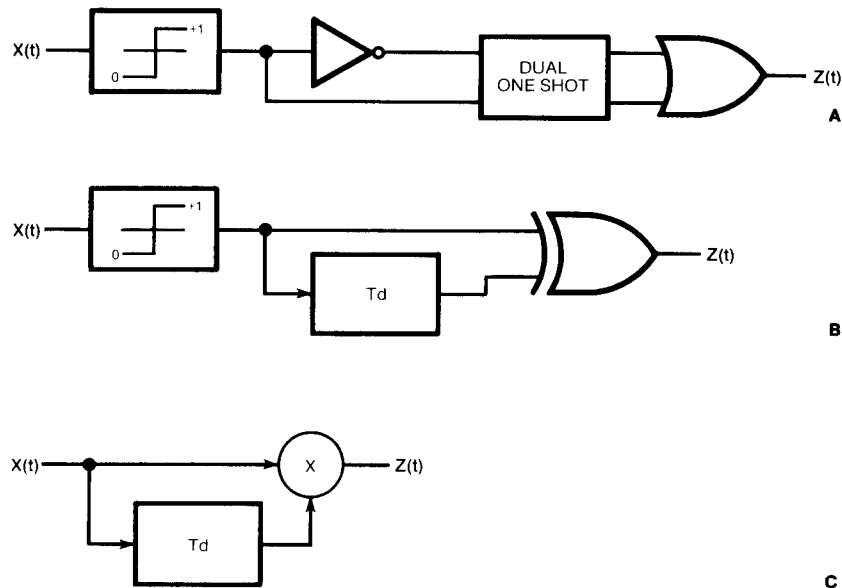


Figure 2. Practical nonlinear processors (A and B: threshold detectors; C: delay and multiply)

To complete the STR, the desired spectral line at

$$f = 1/T_s$$

must be recovered, while residual spectra is suppressed to minimize timing jitter. High data-rate systems will opt for straight-forward bandpass filtering over a PLL to eliminate loop feedback time delays, which would aggravate acquisition time. However, a PLL is often used as a compromise between reasonable acquisition characteristics and excellent filtering tracking performance for moderate baud-rate systems.

An STR narrowband filter employing an analog PLL is shown in Figure 3. The prefilter is excited with a pulse train derived from the raw data stream. Any missing pulse transitions between two adjacent time slots, as in a series of consecutive “ones” or “zeros,” will be interpreted by the loop as a gross frequency error for which the VCO tries to compensate. This results in a hunting effect which prevents the loop from locking to the nominal clock frequency. The prefilter is used to introduce these missing pulse transitions [12]. A prefilter is simply a high-Q filter that, upon loss of input (transitions), will continue to oscillate (ring) at the desired clock frequency

$$f = 1/T_s$$

for a few clock periods. This electrical flywheel allows the PLL to remain locked.

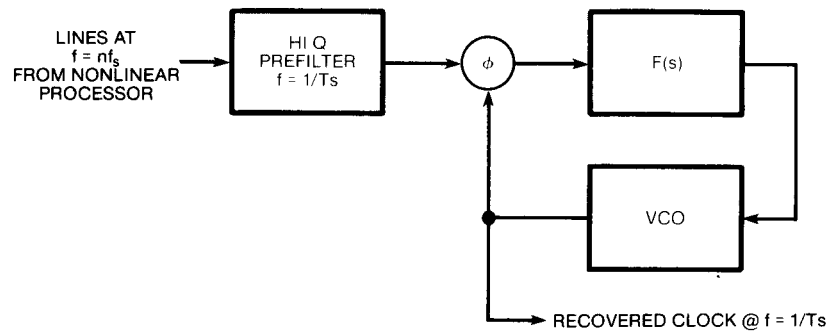


Figure 3. STR narrowband filter employing an analog PLL.

A method of filtering tracking which is moderately insensitive to data transition loss is that of the digital phase-locked loop, or DPLL, which allows discrete phase adjustment of the output clock frequency. Since there are many variations of DPLLs, only one, the (LL)-DPLL, will be described in any detail; a survey of variations is provided in [13].

The lead lag DPLL or (LL)-DPLL has been analyzed by Cessna [14], and forms the basis of a commercially available IC, the Texas Instruments SN74LS297. **[These are still commercially available as of August 2000 (!) --Ed.]** Model block diagrams are shown in Figure 4.

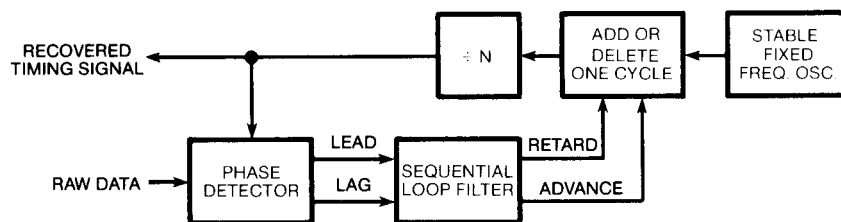


Figure 4A. The (LL)-DPLL.

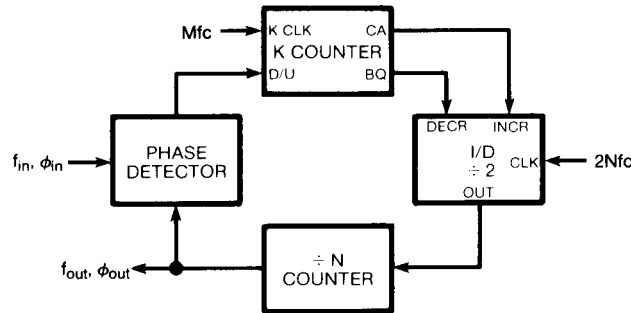


Figure 4B. T.I. SN74LS297 block diagram.

Basic circuit operation is as follows: The incoming data stream (raw data) is phase-compared with a divided-down clock reference. Sequential loop filtering is performed by the K-counter, which is steered via the phase detector to count up from zero to K or down from K to zero. The stochastic process which describes the K-counter output is termed, *random walk*. Carry or borrow pulses are generated when the K-counter recycles, and are used in conjunction with the increment-decrement circuit to add or delete one-half cycle from the ID output. In this way, the frequency (f_{out}) and phase (ϕ_{out}) are continuously adjusted in discrete steps. Loop parameters such as bandwidth and center frequency can be adjusted by the judicious selection of clock reference frequencies and divider moduli. A complete description of the TI 5N74L5297, including pertinent design equations, can be found in reference [15]. A digital PLL should be considered for low baud-rate STR.

Channel Filtering

The last major factor degrading demodulator performance is *intersymbol interference*, or ISI, a term used to describe pulse smearing between time slots in a band-limited channel. Consider the idealized impulse response at the output of the data channel as the summation of

$$\frac{\sin x}{x}$$

waveforms, as depicted in Figure 5. Clearly, if hit sampling occurs at multiples of T_s seconds, the $\sin x/x$ waveshape guarantees that adjacent pulse "tails" pass through zero; i.e., zero ISI. Noting the Fourier pair relationship shown in Figure 6, it is seen that the optimal impulse shaping filter is that of an unrealizable ideal low-pass filter.

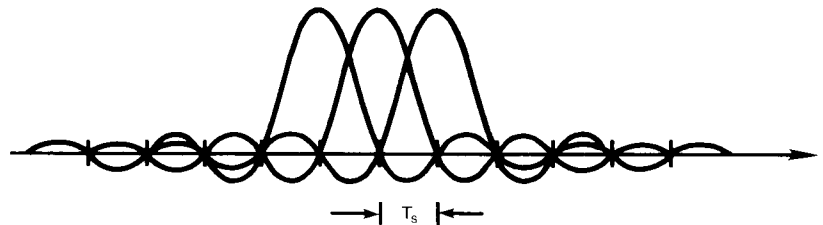


Figure 5. Ideal impulse response.

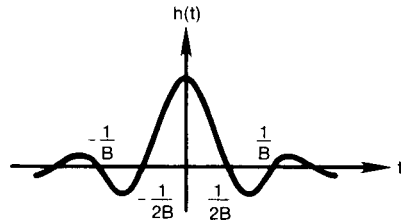


Figure 6A. Desired data channel impulse response.

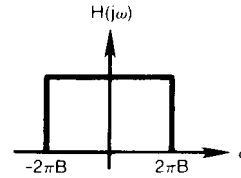
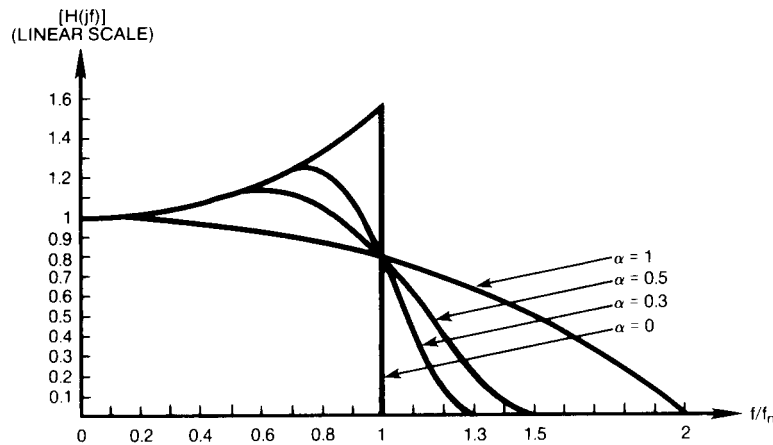


Figure 6B. Required filter.

Nyquist developed criteria for realizable filters which ensure controllable zero crossings. One commonly used class is that of the raised cosine family, shown in Figure 7 with the required

$$\frac{x}{\sin x}$$

amplitude equalization necessary for pulse transmission [2].



$$H(j\omega) \begin{cases} \frac{(\omega T_s/2)}{\sin(\omega T_s/2)} & 0 \leq \omega \leq \frac{\pi}{T_s} (1 - \alpha) \\ \frac{(\omega T_s/2)}{\sin(\omega T_s/2)} \cos^2 \left\{ \frac{T_s}{4\alpha} \left[\omega - \frac{\pi(1 - \alpha)}{T_s} \right] \right\} & \frac{\pi}{T_s} (1 - \alpha) \leq \omega \leq \frac{\pi}{T_s} (1 + \alpha) \\ 0 & \omega > \frac{\pi}{T_s} (1 + \alpha) \end{cases}$$

$\theta(j\omega) = -\omega\tau$ LINEAR PHASE

FROM FEHER WITH PERMISSION © 1981 PRENTICE HALL

Figure 7. Nyquist channel-pulse transmission.

The raised-cosine filters are parameterized by a roll-off factor, α , which can vary from zero, the ideal LPF case, to one for full raised-cosine shaping. For a desired pulse rate

$$2B = B_T = R_s (1 + \alpha)$$

where, R_s = pulse rate in symbols/sec

B = single-sided baseband bandwidth in hertz

B_T = single-sided double-sideband rf bandwidth in hertz

α = roll-off factor $0 < \alpha < 1$

If adjacent channel interference requirements are strict, the designer has only two parameters available for adjustment. The symbol rate can be reduced, resulting in decreased link efficiency, or the roll-off factor can be decreased, resulting in increased filter design complexity.

Although the expressions for optimal pulse shaping were given at baseband, the designer has the option of channel filtering at IF via an LP-BP transformation. Both techniques, while equivalent, lead to different hardware implementations.

Filtering at IF

Quite often the required amplitude response is approximated by a conventional passive filter; e.g., Butterworth, Gaussian, elliptic, followed by group delay equalization, as shown by Figure 8.

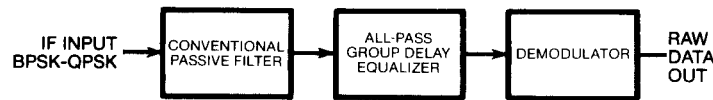


Figure 8. Nyquist filter approximation.

All pass filters, such as the bridged-tee network, are used to flatten the group delay in the passband. This is tantamount to ensuring linear phase, since

$H(j\omega) = |H(j\omega)| e^{-j\omega\tau}$
for a linear phase network

$$\theta(j\omega) = -\omega\tau$$

$$\text{Group delay} = \frac{-d\theta}{d\omega} = \tau$$

a constant

Typically, these channel filters are designed using a CAD program, and are iteratively optimized to a prescribed group delay roll-off factor requirement. Typical systems usually require multi-pole filters and several stages of equalization.

Another method of pulse shaping involves the use of surface acoustic wave (SAW) filters. The basic SAW filter consists of a piezoelectric substrate upon which fingered metalized transducers have been implanted. These transducers serve as converters between electrical and acoustic signals. By varying the spacing, length, and width of the transducer fingers, the impulse response can be carefully controlled. Advantages of SAW filtering include direct analysis in the time domain, linear phase, flexible fractional bandwidths, small size, and high repeatability.

Filtering at Baseband

Baseband channel filtering techniques, mentioned only in passing, are transversal filtering and digital (FIR) filtering. These techniques are prevalent in low-speed demodulation systems and those which are computer intensive. Both methods require a somewhat lengthy explanation; the interested reader is referred to the literature, [16, 17, 18].

ISI Degradation Measurement

A simple but effective method of measuring the peak intersymbol interference degradation of a band-limited channel is by examining its eye diagram [19]. The test setup is shown in Figure 9.

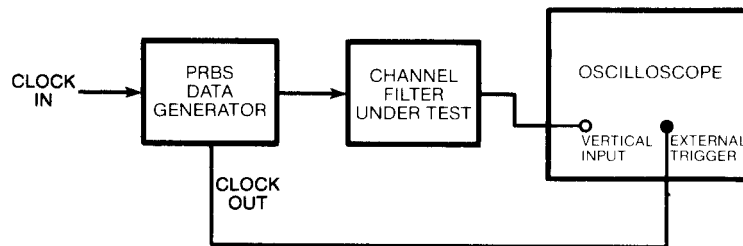


Figure 9. ISI degradation measurement test setup.

The symbol clock is used as the external trigger, while the horizontal time base is adjusted so that one symbol period is displayed. The eye pattern of a band-limited channel will have the form of that shown in Figure 10. The amount of peak ISI distortion is calculated as

$$20 \log_{10} \frac{X}{Y} \text{ (dB)}$$

The magnitude of this value is the increase in E/N_0 ratio required to compensate for the band-limiting effects of the filter.

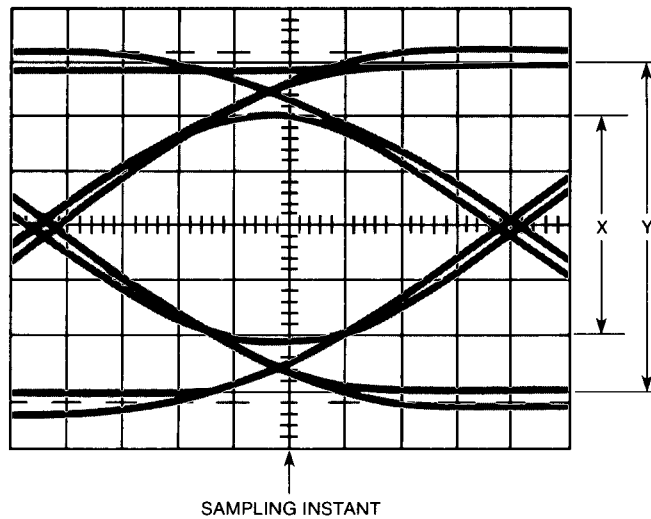


Figure 10. Measured eye diagram of an unequalized filter.

Performance Testing

One standard of demodulator performance is bit error rate, or BER, which is defined as

$$\text{BER} = N_E/N_T$$

where,

N_E is the number of detected bits which are in error and N_T is the total number of bits in the measurement gating period.

Under the common assumption of an additive white gaussian-noise channel (AWGN), very definitive statements can be made concerning theoretical error rates for PSK systems [1, 20]. Of fundamental importance is the result

$$P(e) = \frac{1}{2} \operatorname{erfc} \sqrt{\frac{E}{N_0}}$$

where,

$P(e)$ is the system probability of error, (BPSK-QPSK)
[E is the energy/bit = signal power / bit rate. $-Ed$.]

$$\operatorname{erfc}(x) \triangleq \frac{2}{\sqrt{\pi}} \int_x^{\infty} e^{-y^2} dy$$

the complementary error function

N_0 = the noise spectral density or total noise power in a one-hertz bandwidth

This relationship is plotted in Figure 11. Demodulator performance can be determined by measuring the required E/N_0 for a desired error rate, and comparing this value to theoretical. The difference in E/N_0 is the penalty incurred due to carrier recovery and STR circuitry losses and intersymbol interference.

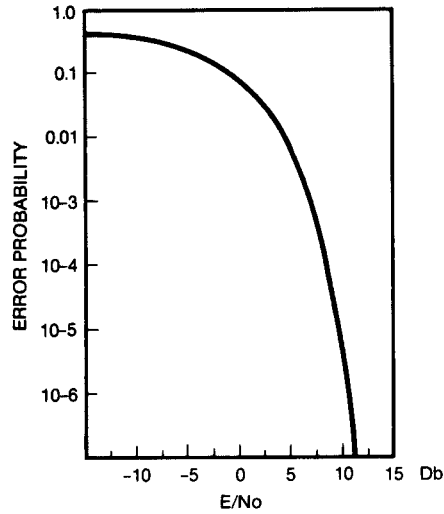


Figure 11. Ideal P(e) curve (BPSK-QPSK)

A typical test setup for BER measurement is shown in Figure 12.

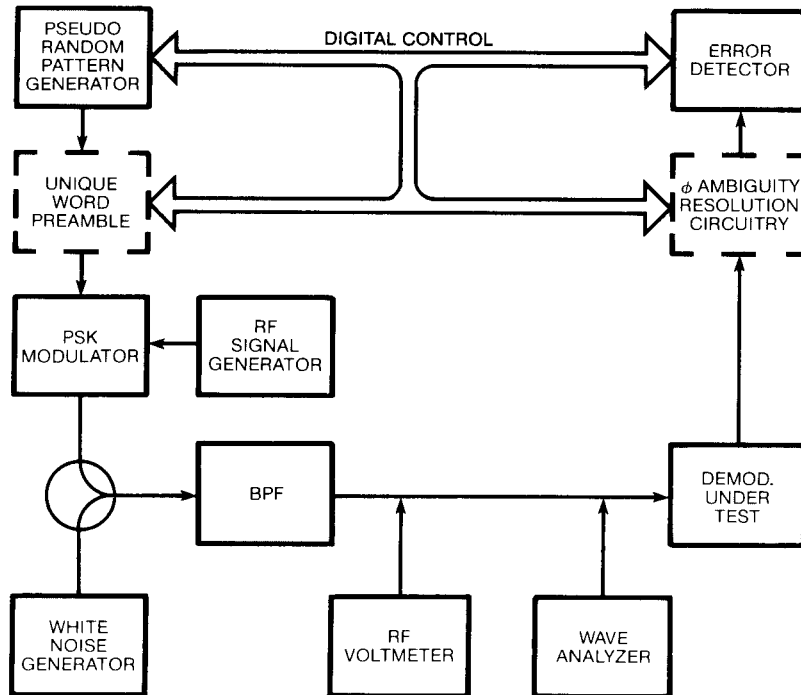


Figure 12. Typical test setup for BER measurement.

For BPSK system testing, the pseudo-random pattern generator supplies a known

sequence of ‘ones’ and zeros’ to the modulator. The BPSK output is then combined with noise via the white noise generator, and the noise floor is increased until a specific E/N_o , is measured. Finally, the noisy BPSK signal is applied to the demodulator under test, with the demodulated data routed to the error detector. Phase ambiguity resolution ($\pm 180^\circ$) is usually not a problem, as most commercial error detectors can process both the recovered PRBS DATA sequence, and its complement, DATA. The error detector then counts the bits which are in error, relative to the transmitted sequence, and provides an indication of BER.

QPSK system testing requires additional phase ambiguity resolution circuitry. Typically, a unique word preamble is appended to the PRBS data frame. The preamble is then decoded at the output of the demodulator, and those data lines which are in error are inverted. Finally, the two data lines are multiplexed together, and the composite bit stream is routed to the error detector. The measured demodulator BER can then be compared to the theoretical performance curves.

E/N_o can be measured indirectly at the demodulator input by using the relationship

$$E/N_o = ST_b/N_o = S/N_o R_b$$

$$E/N_o \text{ (dB)} = 10\log_{10}S - 10\log_{10}R_b - 10\log_{10}N_o$$

where. R_b = the bit rate

Signal power can be measured directly in dBm with an RF voltmeter. The spectral density of the noise can be measured in dBm Hz with a wave analyzer.

Conclusion

This two-part article has presented an overview of the various practical techniques used for the demodulation of PSK encoded signals. Many topics have only been touched on, and the reader is referred to the selected PSK bibliography for a sampling of the pertinent literature.

The design of a PSK demodulator requires the blending of RF, analog, and digital circuitry in proportions dictated by system constraints, such as the required baud rate, channel bandwidth, and maximum allowable acquisition time. As noted throughout this article, these constraints suggest certain circuit realizations, some of which have become *de facto* standards. It is up to the designer, however, to select the techniques that will yield superior demodulator performance at a reasonable cost.

Selected PSK Bibliography

1. Schwartz, M., Information Transmission, Modulation, and Noise, McGraw Hill. New York, 1980.

2. Feher, 14., Digital Communications with Microwave Applications, Prentice Hall, New Jersey, 1981.
3. Lindsey. W. C. and Simon, M. K., Telecommunication Systems Engineering. Prentice Hall, New Jersey, 1978.
4. Blanchard. A., Phase Locked Loops. Wiley, New York, 1976.
5. Simon, M. K., and Lindsey, W. C., "Optimum Performance of Suppressed Carrier Receivers with Costas Loop Tracking," IEEE Transactions on Communications. VOL COM-25. No. 2 (Feb. 1977) pp. 215-227.
6. Simon, M. K., "On the Calculation in Costas Loops with Arbitrary Arm Filters." IEEE Transactions on Communications, VOL COM-26. No. 1 (Jan. 1978) pp. 179-183.
7. Ritter, S., "An Optimum Phase Reference Detector for Fully Modulated Phase-Shift Keyed Signals," IEEE Transactions on Aerospace and Electronic Systems, VOL AES-5, No.4, July1969, pp.627-631.
8. Simon, M. K., "Tracking Performance of Costas Loops with Hard-Limited In Phase Channel," IEEE Transactions on Communications, VOL COM-26, No.4, April1978, pp. 420-432.
9. Weber. C. L., "Demod-Remod Coherent Tracking Receiver for QPSK and SQPSK," IEEE Transactions on Communications, VOL COM-28, No. 12. Dec. 1980. pp. 1945-1958.
10. Wolejsza, C. J., and Chakraborty, D., "TDMA Modem Design Criteria," Comsat Technical Review, Volume 9, Number 2A, Fall 1979.
11. Holmes. J. K., Coherent Spread spectrum Systems, Wiley, New York, 1981.
12. Le-Ngoc, T., and Feher, K., "A Digital Approach to Symbol Timing Recovery Systems," IEEE Transactions on Communications, VOL COM-28, No. 12, Dec. 1980, pp. 1993-1999.
13. Lindsey, W. C., "A Survey of Digital Phase Locked Loops," Proceedings of the IEEE, VOL 69, No. 4, April 1981. pp. 410-430.
14. Cessna, J. R., and Levy, Li. M., "Phase Noise and Transient Times for a Binary Quantized Digital Phase-Locked Loop in White Gaussian Noise," IEEE Transactions on Communications, VOL COM-20, No. 2. April 1972, pp. 94-104.
15. Texas Instrument Applications Report, Bulletin SCA-206, "Digital Phase-Locked Loop Design using 5N54 74L5297."

16. Mueller, K. H., "A New Approach to Optimum Pulse Shaping in Sampled Systems Using Time Domain Filters," BSTJ, VOL 52, No. 5, May-June 1973, pp. 723-729.
17. Feher, K., and DeCristofaro, R., "Transversal Filter Design and Application in Satellite Communications, IEEE Transactions on Communications, VOL COM-24, No. 11, Nov. 1976, pp. 262-1268.
18. Oppenheim, A. V., and Schafer, R. W., Digital Signal Processing, Prentice Hall, New Jersey, 1975.
19. Feher, K., Digital Communications — Satellite Earth Station Engineering, Prentice Hall, New Jersey, 1983.
20. Wozencraft, J. M. and Jacobs, I. M., Principles of Communication Engineering. Wiley. New York, 1965.